

# SLOW-WAVE ELECTRODE STRUCTURES FOR THE ESS 2.5 MeV FAST CHOPPER

Michael A. Clarke-Gayther, CLRC RAL, Didcot, United Kingdom,  
Yi-Nong Rao<sup>†</sup>, Dag Reistad, TSL Uppsala, Sweden.

## Abstract

Slow-wave electrode designs for the European Spallation Source (ESS) 2.5 MeV fast beam chopper are described. The proposed meander folded strip-line structures feature a composite ceramic pillar / vacuum dielectric with excellent radiation hard and vacuum compatible properties. Broad-band transmission line properties have been optimised by modelling time dependent electromagnetic fields in the three dimensional, finite element frequency domain (FEFD) MAFIA, and HFSS codes, and in the finite difference time domain (FDTD) CONCERTO code.

## 1 INTRODUCTION

The European Spallation Source (ESS) [1], is the most ambitious of the existing proposals for the next generation of accelerator driven pulsed neutron sources. Stringent beam loss requirements dictate that the chopping field in the 2.5 MeV medium energy transport line (MEBT), rise and fall (1 to 90%, 90 to 1%) within the beam bunch interval of 2.9 ns.

Slow wave (E-field) transmission line structures have demonstrated field transition times in the nanosecond regime [2, 3], and ESS chopping schemes utilising these structures, have been identified [4] and refined [5].

The structures are designed using finite element field modelling codes, where complex geometry, electrical length, and inter-electrode coupling set a practical limit on the computational accuracy of the broad-band properties. Speed of computation and / or accuracy of the computed properties for the proposed structures, have been enhanced, by identifying small repetitive modules, and modelling their properties in the three dimensional finite element frequency domain (FEFD) HFSS, and MAFIA codes, and the finite difference time domain (FDTD) CONCERTO code. Time domain characteristics for the complete structures were analysed in a SPICE based circuit simulator where the complete structures were modelled by linking the repetitive two-port modules in large series arrays.

## 2 SLOW-WAVE ELECTRODE DESIGN

Basic design parameters for the proposed slow wave electrode structures are shown in Figure 1, where partial chopping of beam bunches is avoided by ensuring that the deflecting E-field propagates at the beam bunch velocity.

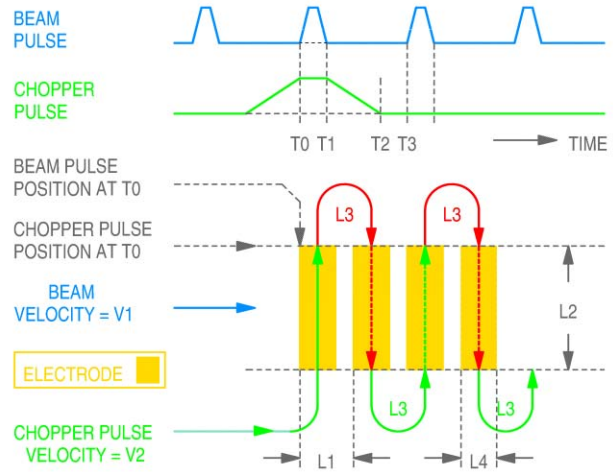


Figure 1: Slow-wave electrode design

In Figure 1:

L2 is the transverse extent of the beam.

T(L1) is the beam transit time for distance L1.

T(L2) is the pulse transit time in vacuum for distance L2.

T(L3) is the pulse transit time in dielectric media (A) for distance L3 and L4 is the electrode width.

For the generalised slow wave structure:

Maximum value for L1 = V1 (T3 - T1) / 2

Minimum Value for L1 = L2 (V1/ V2)

T(L1) = L1/V1 = T(L2) + T(L3)

The relationships for field (E), and transverse displacement (x), where q is the electronic charge, v is the beam velocity, m<sub>0</sub> is the rest mass, z is the effective electrode length, θ is the required deflection angle, V is the deflecting potential, and d is the electrode gap, are:

$$E = \tan \theta \cdot m_0 \cdot \frac{v^2}{q \cdot z}, \quad E = \frac{V}{d}, \quad x = \frac{q \cdot E \cdot z^2}{2 \cdot m_0 \cdot v^2}$$

Inspection shows that for given values of m<sub>0</sub>, v, and V, large θ and x are obtained when z is large and d is small. The inter-electrode gap, shown as L1-L4 in Figure 1, must be made significant if pulse distortion (dispersion) due to inter-electrode coupling is to be minimised.

For a given overall structure length, the effective length (z) will therefore, be maximised, by maximising the electrode width (L4).

<sup>†</sup> Now at TRIUMPH, Vancouver, BC, Canada.

### 3 CANDIDATE ELECTRODE STRUCTURES

Two, candidate, slow-wave structures are presented. Both structures feature a vacuum dielectric, strip-line configuration near the beam axis. The dispersive effect of inter-electrode coupling has been minimised in these designs by ensuring that coupling occurs only in a region near the beam axis. Key parameters, common to both designs, are listed in table 1.

Table 1: Key Parameters

Beam velocity	$v$	2.184e7	m.s <sup>-1</sup>
Mechanical length		400.0	mm
Effective length	$z$	294	mm
Electrode to beam axis gap	$d$	6.0	mm
Beam aperture		11.0	mm
Deflection angle	$\theta$	16	mr
Deflection potential ( $\pm$ )	$V$	1.6	kV
Characteristic impedance	$Z_0$	50 $\pm$ 0.5	$\Omega$
Total structure delay		18.04	ns
No. of sections		21	
Section delay	T(L1)	0.87	ns
Pulse transition time (1-90, 90 -1%)		2.9	ns
Pulse duration (fwhm)		8.0	ns
Pulse aberration (droop / overshoot / reflections)		< 2 %	pulse max.
Structure bandwidth		0.2 - 500	MHz
Section pitch	L1	19.0	mm
Strip-line width	L4	14	mm
Strip-line thickness		0.5	mm

#### 3.1 Electrode structure A

A mechanical schematic of electrode structure A is shown in Figure 2, where the planar strip-line structure is supported at intervals, on ceramic pillars in vacuum. Thin walled separators extend full height, and minimise inter-electrode coupling. Strip-line bends and

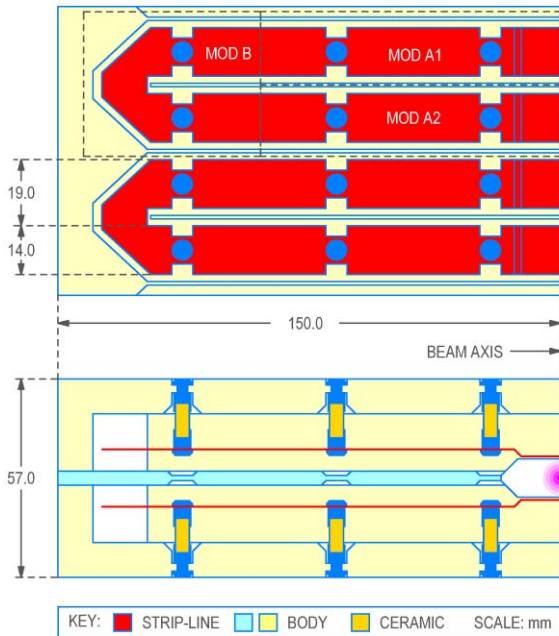


Figure 2: Electrode structure A

supports are capacitively compensated by mitre and notch dimensioning, respectively. A central grounded plate extends full length, and minimises upper to lower electrode coupling.

Finite element models for two modules, identified as MOD A1/A2 and B1 in figure 2, were analysed. Simulated S-parameters for the modules are shown in Figure 3.

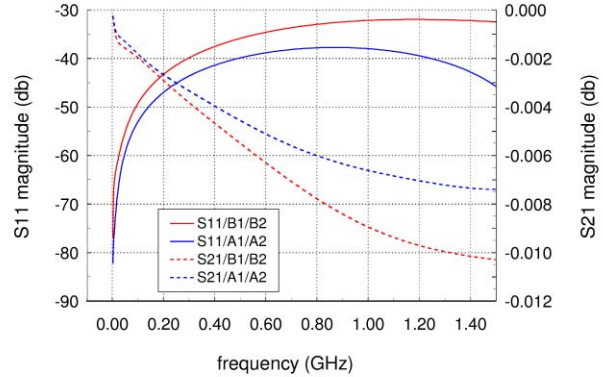


Figure 3: Structure A / Module S-Parameters

Time and frequency domain characteristics for the complete structure were computed by circuit simulation of series connected, two port modules, and lumped element inter-electrode, coupling capacitors, as shown in Figure 4.

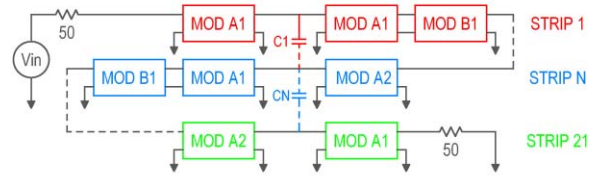


Figure 4: Structure A / SPICE model

The simulated pulse transmission characteristics for the complete structure are shown in Figure 5. Comparison with the structure B response, as shown in Figure 9, suggests that structure A exhibits lower transmission loss and less pulse shape distortion, but that the characteristic impedance is not as tightly controlled. Overshoot and undershoot are shown to be a function of inter-electrode coupling capacitance. This effect is more pronounced for the higher bandwidth structure A, than for structure B.

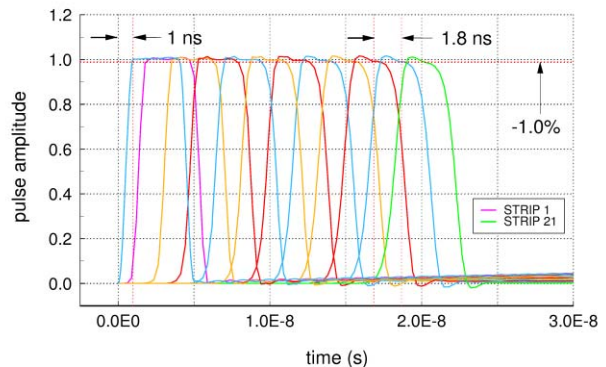


Figure 5: Structure A / Transient Response

### 3.2 Electrode structure B

A mechanical schematic of electrode structure B is shown in Figure 6, where the compact helical structure is formed by strip-line sections near the beam axis, linked by semi-circular sections of semi-rigid coaxial cable (UT-390). Coaxial to strip-line transitions, and ceramic strip-line supports, are capacitively compensated by structure and notch dimensioning, respectively.

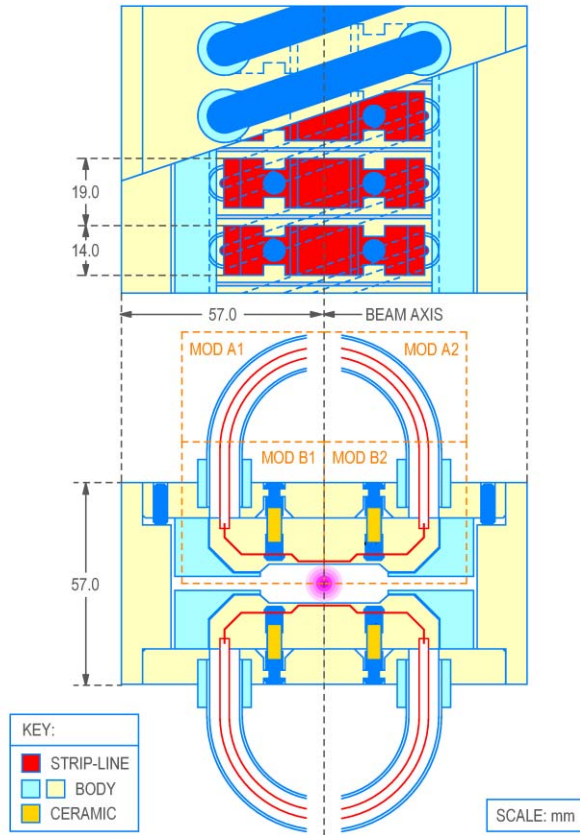


Figure 6: Electrode structure B

Finite element models for two modules, identified as A1/A2 and B1/B2 in Figure 6, were analysed. Simulated S-parameters for the modules are shown in Figure 7, where the S<sub>21</sub>/A1/A2 for the coaxial cable shows good agreement with manufacturers' data.

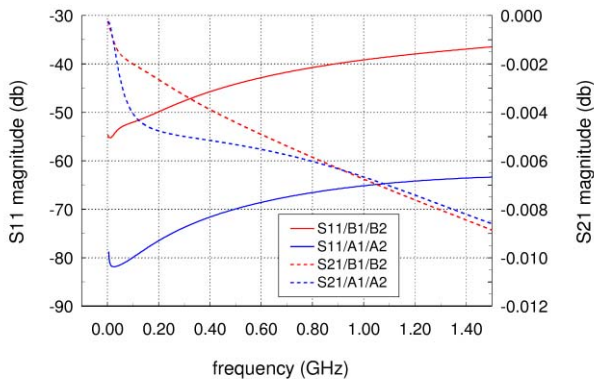


Figure 7: Structure B / Module S-Parameters

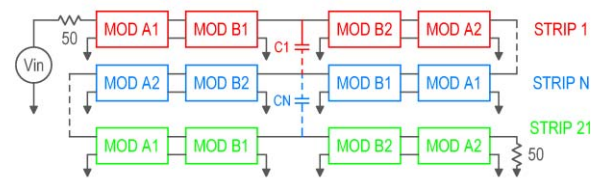


Figure 8: Structure B / SPICE model

Time and frequency domain characteristics for the complete structure were computed by circuit simulation of series-connected two-port modules and lumped element inter-electrode coupling capacitors, as shown in Figure 8. The simulated pulse transmission characteristics for the complete structure are shown in Figure 9.

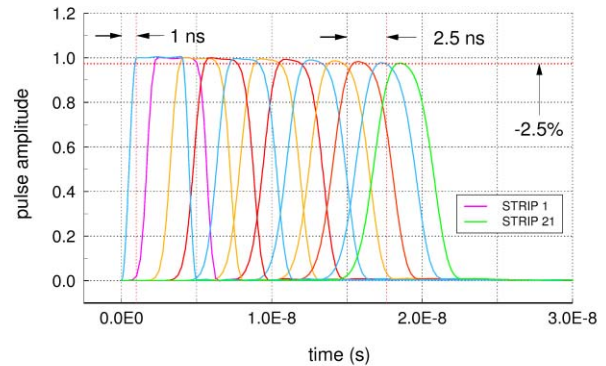


Figure 9: Structure B / Transient Response

## 4 SUMMARY

Slow-wave electrode structures for the ESS 2.5 MeV beam chopper have been modelled using finite element and circuit simulation codes. The computed frequency and time domain characteristics indicate that the candidate structures may meet the required specifications for chopper pulse fidelity. Speed of computation and / or accuracy of computed properties have been enhanced by the analysis of repetitive modules and inter-electrode coupling elements in a circuit simulation code.

## 5 REFERENCES

- [1] The ESS Accelerator and Beam Lines with the 280/560 MHz Linac, Report No. ESS-01-1A, December 2001.
- [2] S. S. Kurennoy, and J. F. Power, 'Development of Meander-Line current structure for SNS fast 2.5 MeV Beam Chopper', Proc. of the 7th European Particle Accelerator Conference, Vienna, Austria, June 2000, p.336-338.
- [3] J. S. Lunsford and R. A. Hardekopf, 'Pulsed beam chopper for the PSR at LAMPF', IEEE Trans. Nucl.Sci., NS-30, 1983.
- [4] M. A. Clarke-Gayther, 'Modulator Systems for the ESS 2.5 MeV Fast Chopper', Proc. of the 2001 Particle Accelerator Conference, Chicago, USA, p. 4062-4065.
- [5] M. A. Clarke-Gayther, 'A Fast Chopper for the ESS 2.5 MeV Beam Transport Line', this conference.